Journal of the Meteorological Society of Japan, Vol. 78, No. 3, pp. 223–231, 2000

The Influence of the Moisture Gradient on the Accuracy of Precipitable Water Derived from GPS data

By Hiroyuki Iwasaki

Faculty of Education, Gunma University, Maebashi, Japan

Fujio Kimura

Institute of Geoscience, University of Tsukuba, Tsukuba, Japan

Kiyotaka Nakagawa

Division of Science, Joetsu University of Education, Joetsu, Japan

Takahiro Miki

Faculty of Education, Gunma University, Maebashi, Japan

Fumiaki Kimata

School of Science, Nagoya University, Nagoya, Japan

Seiichi Shimada

National Research Institute for Earth Science and Disaster Prevention, Tsukuba, Japan

and

Shigeru Nakao

Earthquake Research Institute, The University of Tokyo, Tokyo, Japan

(Manuscript received 24 August 1999, in revised form 10 February 2000)

Abstract

One of the major sources of the error in estimating precipitable water derived from GPS data is horizontal gradient of the moisture. Several characteristics of the error were investigated in comparison with water-vapor radiometer measurements.

The GPS-precipitable water (GPS PW) exhibited good agreement with precipitable water derived from water-vapor radiometer measurements. The correlation coefficient and rms error for this comparison were determined as 0.991 and 1.93 mm, respectively.

The estimation errors for the GPS PW can be divided into two components based on the time scale of the variation. The first components of the error has low frequency with the time scale of several days, with an amplitude of about 2.5 mm. This estimation error was negatively correlated with the north-south component of the GPS-PW gradient derived from GPS data. The GPS PW was overestimated under the condition in which water vapor increased southward.

Corresponding author: Hiroyuki Iwasaki, Department of Earth Science, Faculty of Education, Gunma University, 4-2, Aramaki, Maebashi, 371-8510, Japan. E-mail: iwasaki@edu.gunma-u.ac.jp

Another component of the error has high frequency with the time scale of several hours, having an amplitude of at most 5.0 mm. The high frequency component of the error seems to depend on rapid changes of the GPS-PW gradient.

1. Introduction

Mesoscale variations of water vapor caused by the thermally induced local circulation are important in order to understand the behavior of cumulonimbus clouds. It had been rather difficult, however, to observe the mesoscale distribution of precipitable water (PW) over land with sufficient accuracy. In recent years, the PW over land has been retrieved from the electrical wave signal data from Global Positioning System (GPS) satellites, with high time resolution and high accuracy (e.g., Bevis et al. 1993, 1994; Rocken et al. 1995).

The Geographical Survey Institute (GSI) of Japan has deployed 947 geodetic GPS receivers in a dense network across Japan, with a resulting spatial resolution of about 20 km. The GPS PW derived from the GSI-GPS network has sufficient resolution to clarify the features of mesoscale disturbances. However, the delay of electrical wave signals due to atmospheric moisture is calculated from GPS data under the assumption of a uniform horizontal distribution of water vapor. The local circulation, induced by the thermal imbalance between the plain and mountains, causes diurnal variations of water vapor (Kimura and Kuwagata 1993, 1995). The range of the diurnal variation of PW frequently reaches values over 10 mm at Gunma University located in a semi-basin (Iwasaki and Ohbayashi 1998; Iwasaki 1999). In the daytime hours of summer sunny days, water vapor is transported from the plain to the mountains, and during the nighttime to early morning, in the opposite direction (Kimura and Tanikawa 1997; Iwasaki 1999). This means that the moisture gradient around mountainous areas is reversed between daytime and nighttime.

It is well known that geodetic parameter estimations are affected by the horizontal moisture gradient (e.g., Ichikawa et al. 1995, 1996; Kimata et al. 1996; Alber et al. 1997; Kimata and Mannoji 1998). There is a possibility that the moisture gradient also creates noise in the GPS PW in the region where diurnal variations of water vapor are prominent. The purpose of the present study is to clarify the relationship between the errors in estimating the GPS PW and the horizontal moisture gradient, to advance applications in mesoscale meteorology.

2. Data and analysis of GPS data

2.1 Observation

The observational period was from 20 July to 24 August, 1998. Figure 1 shows the location of the observational sites. In order to determine the gradient of precipitable water, three GPS receivers were triangularly installed at Kizaki (KIZA), Numata (NUMA), and Kurabuchi (KURA). A GPS receiver and a water-vapor radiometer (WVR) were placed at Gunma University (GUNU), located in the center of the triangular network. A total of 25 radiosondes were launched from the same site from 20 July to 4 August, in order to calibrate the WVR PW . Surface temperature and pressure were also observed at GUNU within an accuracy of 0.1 K and 0.1 hPa, respectively, in order to calculate the GPS PW from total zenith delay (TZD).

The summer season of 1998 over the Kanto district was the so-called "cold summer", in which the thermally induced local circulation did not develop. The variations of water vapor and its gradient determined in the present paper are therefore associated with synoptic scale disturbances.

2.2 Procedure to calculate the GPS and WVR-precipitable water

The properties of the GPS analysis are listed in Table 1. The GPS receivers collected all data from GPS satellites above 15 degrees elevation at a 30-second interval. The GPS PW is estimated from the values of TZD, which are directly calculated from the GPS data every 30 minutes with the use of Bernese GPS software Version 4.0, using measurements of surface temperature and pressure at GUNU.

The TZD is the atmospheric delay of the GPS signal arriving from the zenith direction, and can be separated into two components: the zenith hydrostatic delay, and the zenith wet delay. The zenith hydrostatic delay can be estimated from the surface pressure. After removing the zenith hydrostatic delay from the TZD, the remaining zenith wet delay is nearly proportional to the precipitable water. The proportional factor slightly depends on the weighted mean temperature of the atmosphere T_m. In the present study, T_m is estimated from surface temperature data by the regression formula (see, Table 1) as proposed by Bevis et al. (1994).

Surface temperature and pressure at KIZA, NUMA, and KURA were estimated from data observed at GUNU, assuming hydrostatic equilibrium and a constant temperature lapse rate of 6.5 K/km. The horizontal variations of temperature and pressure were neglected, since the scale of network was small.

The WVR measures microwave radiation emitted from the atmosphere and obtains a brightness temperature. The emission from raindrops also contributes to the brightness temperature, which creates noise in the water vapor measurement. When

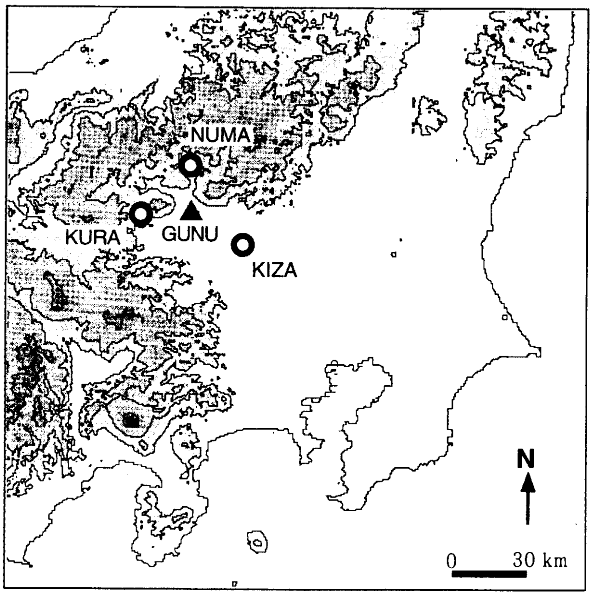

O : GPS receiver

▲ : GPS + WVR + Sonde+Meter. observation

Fig. 1. Location of the GPS and WVR sites. The elevation is indicated by the degree of shading. The counter interval is 500 m.

Table 1. Properties of the GPS analysis.

Software	Bernese version 4.0
Sampling rate	30 seconds
Cutoff angle	15 degrees
Remote GPS sites	Shanghai, Fairbanks, Guam, Irkutsk
Time resolution of TZD	30 minutes
Mapping function	1/cos (zenith angle)
Tm	Tm=70.2+0.72*Tsfc

the liquid-water content derived from the WVR measurements exceeded 0.10 mm, the data were eliminated to avoid any contamination by the raindrops. Further, the WVR PW was calibrated using the precipitable water derived from 25 radiosondes observation in order to remove a large bias in WVR data. The correlation coefficient and rms error between the calibrated-WVR PW and sonde PW were 0.923 and 1.65 mm, respectively. The calibrated-WVR PW was then averaged every 30 minutes in order to adjust to the time resolution of the GPS PW.

2.3 Difference between GPS PW and WVR PW

Figure 2a schematically illustrates the beamwidth of the WVR and GPS receiver. The WVR observes water vapor only near the zenith point, due to the narrow beamwidth of about 5 degrees. On the other hand, since the cutoff angle of the GPS receivers is 15 degrees, the GPS observes water vapor within a volume of an upended right circular cone, having a vertex angle of 150 degrees (see Fig. 2a). Assuming the scale height of water vapor as 3.5 km, the GPS PW represents the averaged precipitable water over a radius of about 13 km.

Figure 2b schematically illustrates the gradient of precipitable water over a GPS receiver. The orbit inclination of GPS satellites is 60 degrees, so that many satellites concentrate on the southern sky as illustrated in Fig. 2b. Therefore, water vapor in the southern atmosphere may be emphasized than that in the northern atmosphere. Further, the mapping function in the Bernese software version 4.0 is based on the assumptions that the atmosphere above GPS sites is azimuthally isotropic and stationary. Therefore, the precipitable water derived from GPS data will be affected by the horizontal moisture gradient and its variations, which differs from the WVR derived PW.

Besides the moisture gradient, since Bernese GPS software version 4.0 does not include ocean loading effect, the vertical displacement of GPS sites due to ocean loading also influence the accuracy of the GPS PW. Shoji et al. (1999) indicated that the ocean loading effects on the local GPS site and remote GPS sites cause the estimation error of 4 mm at most. Since the vertical displacement is 2 cm even in the coastal region, the ocean loading effect does not influence the WVR-PW estimation. However, the main estimation errors due to the ocean loading have periods of about 24 and 12 hours, so that these errors can be regarded as random noise with respect to variation of the moisture gradient associated with synoptic disturbances.

3. Definition of the water-vapor gradient and estimation errors

The water-vapor gradient was calculated from the GPS PW at KIZA, NUMA, and KURA (see Fig. 1). The water-vapor gradient, however, cannot be exactly determined, due to differences in the elevation among the three GPS sites being as much as 400 m. Therefore, firstly, GPS-PW anomaly (PW′) were determined for three GPS sites. Secondly, the east-west component ($\frac{\partial PW'}{\partial x}$) and north-south component ($\frac{\partial PW'}{\partial y}$) of the gradient of the GPS-PW anomaly were determined for the triangular GPS network. For simplicity, these components are termed the E–W and N–S components of the GPS-PW gradient.

As was mentioned in the previous section, comparisons of GPS PW are made with WVR as an accurate independent measurement. Any estimation errors in the WVR measurements will be neglected in order to simplify the problem. In this paper, the difference between the GPS PW and the calibrated-WVR PW (GPS PW minus WVR PW) is defined as the estimation error resulting from the moisture gradient.

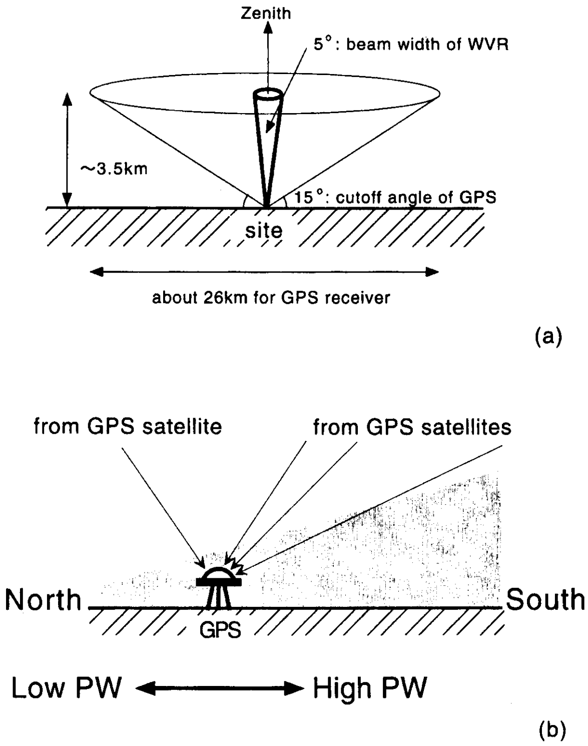

Fig. 2. Schematic illustration of the beamwidth of the GPS and WVR (a) and the gradient of precipitable water over a GPS receiver (b). The thin line arrows indicate electric wave signals from GPS satellites. The shading indicates a moist layer in the lower atmosphere.

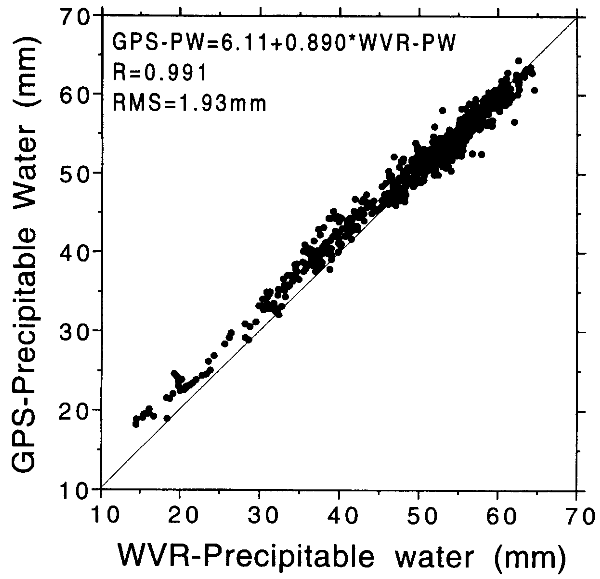

Fig. 3. Scatter diagram of the calibrated-WVR PW versus the GPS PW observed at GUNU.

4. Results

4.1 Comparison of GPS PW and the calibrated-WVR PW

Figure 3 displays a scatter diagram between the GPS PW and the calibrated-WVR PW results observed at GUNU. The correlation coefficient and rms error are 0.991 and 1.93 mm, respectively. The GPS PW exhibits good agreement with the the calibrated-WVR PW, as was reported in the previous studies (e.g., Duan et al. 1996; Ohtani et al. 1997; Shoji et al. 1999; Ohtani 1999). In spite of the high correlation, however, there are a number of considerable estimation errors. In the next section, these errors will be classified according to the time scale of the variations.

4.2 Two components of estimation errors

Figure 4 shows the time sequence of the calibrated-WVR PW at Gunma University (a), and the gradient of the GPS-PW anomaly derived from the GPS triangular network (b and c). The E–W and N–S gradients of the GPS-PW varied within 0.3 mm/km, and histograms for both components exhibit almost normal distributions (Fig. 5). The E–W and N–S gradient tend to change with the same phase from 31 July to 15 August, but it is difficult to recognize any clear correlation between them prior to 29 July and after 16 August. These phase relationships would be caused by anisotoropic variability of the horizontal moisture pattern associated with synoptic disturbances.

Figure 4d shows the time sequence of the estimation error, which varied from −7 mm to +6 mm. Since the variation of estimation error is enough larger than the rms error between the calibrated-WVR PW and sonde PW of 1.65 mm, any estimation errors of WVR and sonde were not a major source of the estimation error in the GPS PW.

The variation of the error seems to have two components with a different time scale, one is several days and another is several hours. These errors have several features, as described in the following.

4.2.1 Estimation error varying with several days

The estimation error of the GPS PW varied over several days, with an amplitude of about 2.5 mm. It is noted that the time series of the N–S gradient of the GPS-PW is negatively correlated with the estimation error throughout the observational period. Although the E–W component also exhibits on the negative correlation with the estimation error, the correlation coefficient of −0.224 was less than that of the N–S component ($R = -0.346$, see Fig. 6). In addition, the E–W component was not correlated with the estimation error prior to 29 July and after 16 August. Therefore, attention will be focused on the relationship between the N–S component of the GPS-PW gradient and the estimation error varying over several days.

Figure 6a and 6b show scatter diagrams of the estimation error and the components of the GPS-PW gradient. The estimation error is roughly correlated with the N–S component of the GPS-PW gradient.

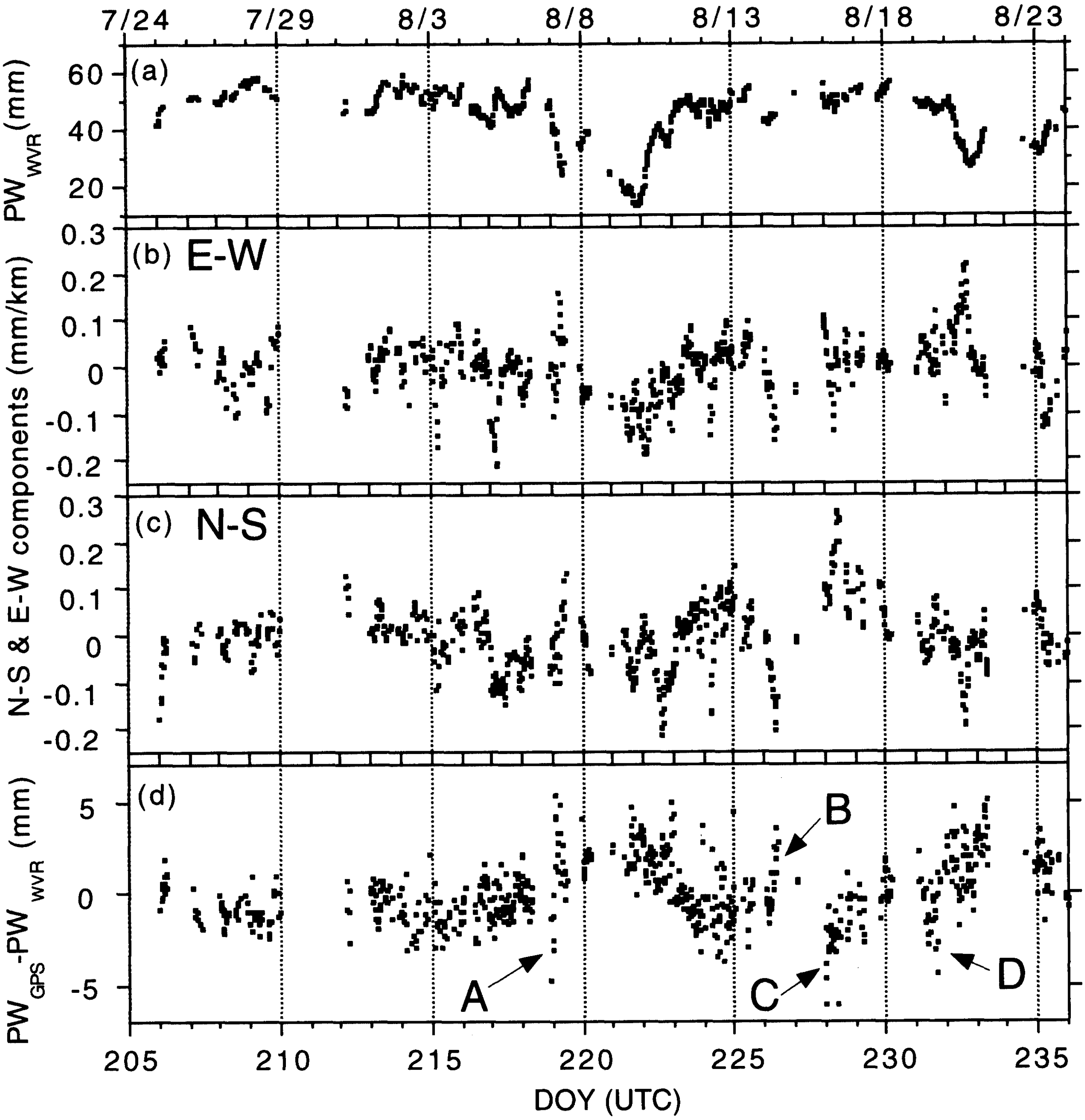

Fig. 4. Time sequence of (a) the calibrated-WVR PW at GUNU, (b) the E–W and (c) the N–S components of the GPS-PW gradient, and (d) the estimation errors of the GPS PW. No data of the calibrated-WVR PW was due to rain contamination. Positive values of the E–W component and N–S component indicate that the GPS PW anomaly increases eastward and northward, respectively. Positive values of the estimation error indicate that the GPS PW was overestimated. Periods labeled A to D indicate rapid changes in the estimation errors.

The correlation coefficient is −0.346, and the regression equation is obtained as in Eq. (1) as

$$PW_{GPS} - PW_{WVR} = 0.727 - 8.56 * \text{N–S component} \tag{1}$$

In spite of the low correlation coefficient, the hypotheses of no correlation is rejected at 0.1 % significance level. Further, this negative correlation is clearer ($r = -0.489$) after 3 August, when the variation of the GPS-PW gradient was large (Fig. 6c). It should be noted that the GPS PW had a tendency to be overestimated when water vapor has a southward gradient, which are well recognized under the low precipitable water as less as 40 mm in Fig. 3.

4.2.2 Estimation error varying over several hours

Another type of estimation error can be clearly seen at period A to D in Fig. 4d. The estimation error changes rapidly over a period of several hours, with the range of the error values reaching 10 mm.

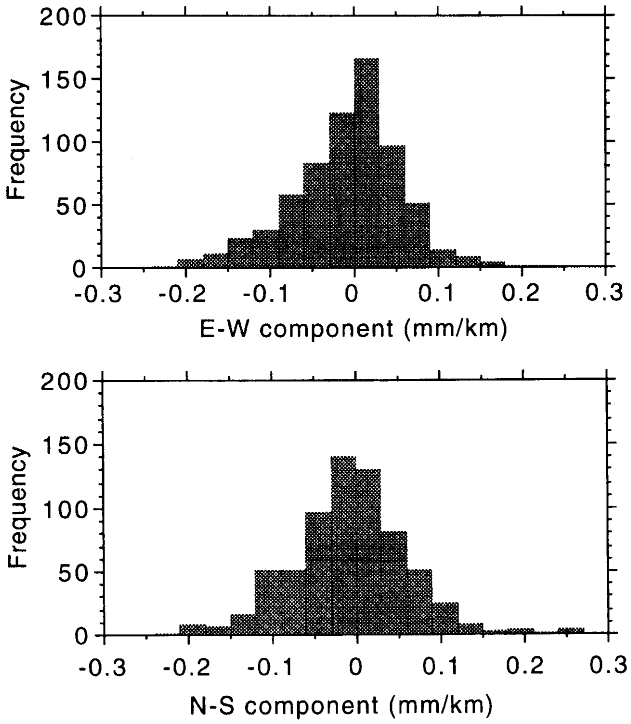

Fig. 5. Histogram of the E–W component (upper) and N–S component of (lower) the GPS-PW gradient.

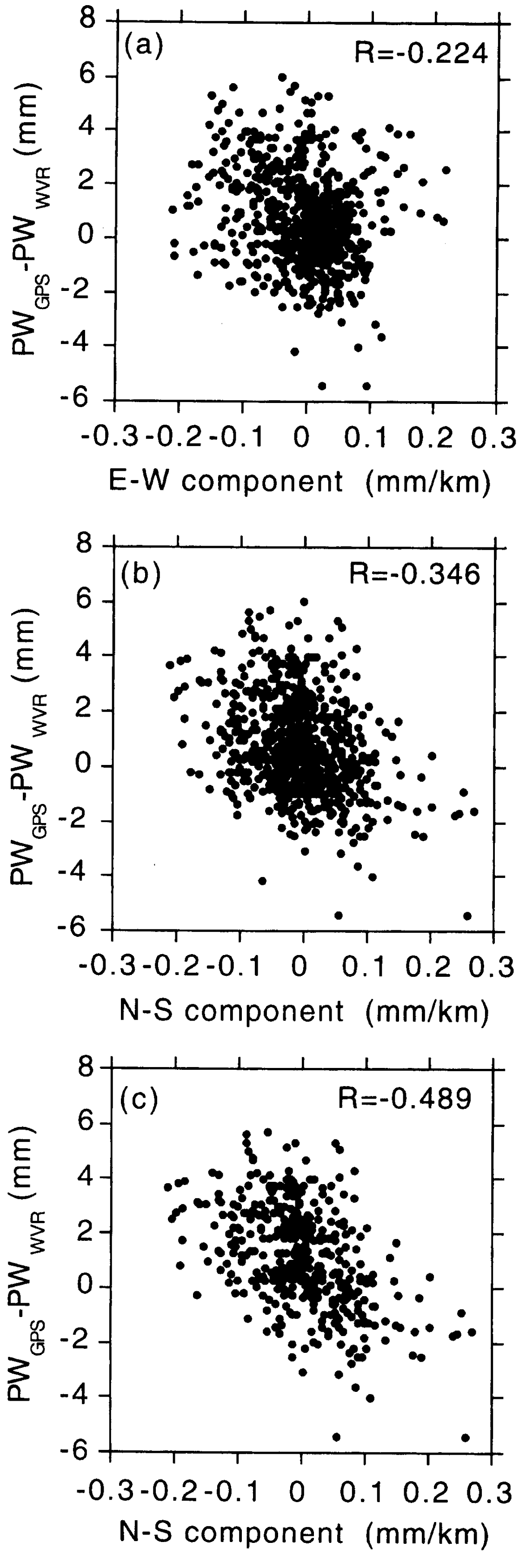

Fig. 6. Scatter diagram of estimation error of the GPS PW versus (a) the E–W component, (b) the N–S component of the GPS-PW gradient, and (c) the N–S component after 3 August.

This estimation error has a different feature from the error varying over several days.

Figure 7 displays the scatter diagram of the estimation error versus the N–S component for periods A to D. Although estimation errors for period B were well correlated with the N–S component of the GPS-PW gradient ($R = -0.731$), other periods A, C, and D fluctuate independently of the GPS-PW gradient. Most of the estimation errors are correlated with rapid changes in the GPS-PW gradient, rather than with the GPS-PW gradient itself.

5. Discussion

5.1 Interpretation of estimation errors varying over several days

Although the estimation of TZD is based on the assumptions that the atmosphere above GPS sites is azimuthally isotropic and in a steady state, the moisture gradient in the actual atmosphere over GPS sites varies (Figs. 4a to 4c). Discussion will now be focused on the relationship between the estimation error and the GPS-PW gradient.

The WVR observes at near the zenith point due to the narrow beamwidth of 5 degrees, so that the influence of the moisture gradient will be small enough to neglect. On the contrary, the beamwidth of the GPS receiver can be regarded as 150 degrees, as illustrated in Fig. 2a. Further, many satellites concentrate on the southern sky, since the orbit inclination of GPS satellites is 60 degrees (Fig 2b). Unlike the WVR, it is considered that the hydrostatic de-

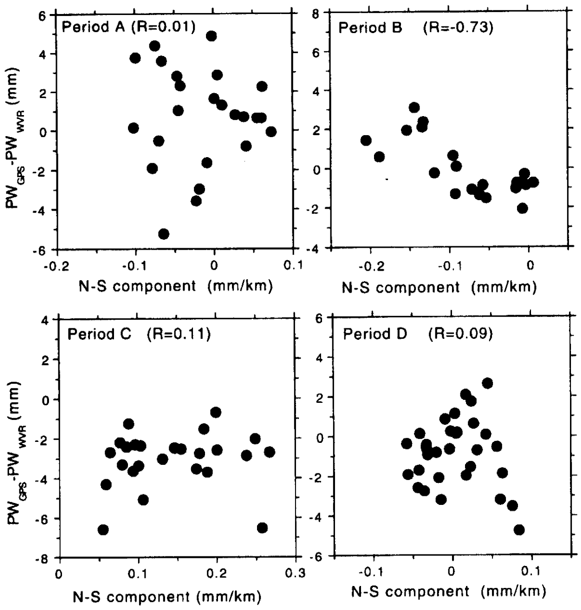

Fig. 7. Scatter diagram of the estimation error versus the N–S component for periods of A to D.

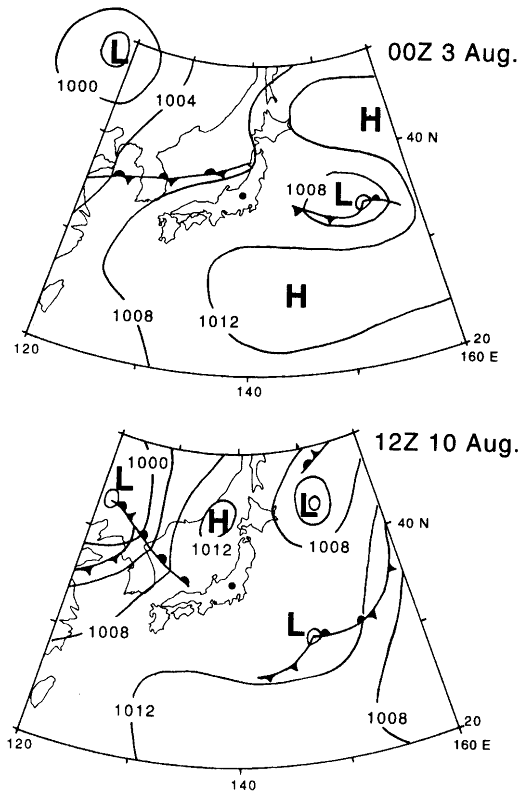

Fig. 8. Surface weather charts at 00 Z 3 and 12 Z 10 August, 1998. (a) Typical synoptic situation when the estimation error varying over the several days was small. (b) Typical synoptic situation when the GPS PW was overestimated. Closed circle indicates the location of GUNU. These weather charts were copied from JMA Weather charts provided by Japan Meteorological Agency (JMA).

lay in the southern atmosphere is emphasized more so than the northern atmosphere. Therefore, GPS PW will be overestimated under conditions in which the water vapor increases southward. This interpretation is consistent with the relationship between the estimation error and the N–S component of the GPS-PW gradient (Fig. 6b and 6c).

The N–S component of the GPS-PW gradient varying over several days depends on synoptic situation. When a stationary front and/or a depression located to the north of the Kanto district, the estimation error was relatively small (Fig. 8a). On the other hand, when a high located in the north of the Kanto district, the GPS PW was overestimated (Fig. 8b). The time scale of change in two synoptic patterns accorded with that of the N–S component of GPS PW. Moisture gradient over the triangular GPS network must have varied as synoptic scale pattern changed, as a result, the estimation error in the GPS PW was varying over the several days.

5.2 Interpretation of estimation errors varying over several hours

A different interpretation for the estimation error varying over several hours must be obtained, since this error varied independently of the GPS-PW gradient derived from the triangular GPS network (Fig. 7). Estimation errors varying over several hours often occurred during the periods of rapid change in the GPS-PW gradient, which is contrary to the assumption used to calculate TZD with the Bernese GPS software Version 4.0, namely that the atmosphere is isotropic and in a steady state. The rapid change in the moisture gradient might cause estimation errors varying over several hours.

Figure 9 shows the location of surface front around Period A. No data of WVR PW prior to the Period A in Fig. 4a was due to rain associated with the front. After the passage of the front over the GPS site, rapid changes in the GPS-PW gradient occurred at 00 Z on 7 August. This argument applies very well to the rapid changes in the GPS-PW gradient of B to D in Fig. 4. Therefore, the passage of mesoscale moisture pattern on the rear site of the fronts must have caused the estimation error varying over several hours.

5.3 Correction of the estimation error varying over several days using the GPS-PW gradient

Since the estimation error varying over several days can be correlated with the large scale moisture gradient, as shown in Fig. 6, the GPS PW at GUNU can be corrected using GPS-PW gradient over the triangular GPS network and the regression equation, Eq. (1).

Table 2 lists the results of the correction. When compared to the results prior to the correction, the corrected regression line approaches the $Y = X$ rela-

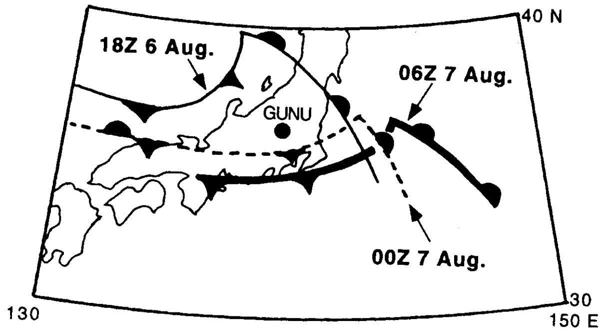

Fig. 9. Location of surface fronts from 18 Z 6 August to 06 Z 7 August, 1998. Closed circle indicates the location of GUNU. The location of fronts were determined using JMA Weather charts.

Table 2. List of regression characteristics without and with the correction using Eq. (1).

	Slope	Interception	R	rms
Without correction	0.890	6.11 mm	0.991	1.93 mm
With correction	0.906	4.56 mm	0.991	1.65 mm

tionship, and the rms error is reduced from 1.93 mm to 1.65 mm. It is reasonable to conclude that this correction improves the accuracy of the GPS-PW at GUNU. The estimation error that varies over several hours, however, still remains. Care must be used when interpreting the GPS-PW variation when the moisture gradient rapidly changes around the GPS site.

6. Summary

Several characteristics of the errors in estimating GPS-precipitable water (GPS-PW) studied in comparison with water vapor radiometer (WVR) measurements, with respect to the horizontal moisture gradient. The following results were obtained:

1. The GPS PW exhibited good agreement with the precipitable water (PW) derived from WVR measurements. The correlation coefficient and rms error were determined as 0.991 and 1.93 mm, respectively.

2. The errors in estimating GPS PW were divided into two components, with respect to the time scale of the variation.

3. The low frequency component of the error, with the time scale of several days and the amplitude of 2.5 mm, is negatively correlated with the north-south component of the GPS-PW gradient. GPS PW is overestimated under the condition in which the water vapor increases southward.

4. The second component of the error has the time scale of several hours with the amplitude of 5 mm at most. The errors were related to the passage of the synoptic scale fronts, and seems to depend on rapid change in the GPS-PW gradient.

Acknowledgments

This research was supported by a grant from the GPS/MET Japan (GPS Meteorology Project in Japan) funded by the Science and Technology Agency of Japan, and in part by the joint research program of CEReS, Chiba University (No.10–16). Thanks are due to staff members of the Kizaki Junior High School, the Numata Elementary School, and the Kurabuchi Elementary School for providing GPS sites. Special thanks are due to staff members of the Water Manage Planning Section of Tone River Dams Integrated Control Office for providing the water-vapor radiometer.

References

Alber, C., R. Ware, C. Rocken and F. Solheim, 1997: GPS surveying with 1 mm precision using corrections for atmospheric slant path delay. *Geophys. Res. Let.*, **24**, 1859–1862.

Bevis, M., S. Businger, S. Chiswell T.A. Herring, R.A. Anthes, C. Rocken and R.H. Ware, 1992: GPS meteorology: Mapping zenith wet delays onto precipitable water. *J. Appl. Meteor.*, **33**, 379–386.

———, ———, T.A. Herring, R.A. Anthes, C. Rocken and R.H. Ware, 1994: GPS meteorology: Remote sensing of atmospheric precipitable water using the Global Positioning System. *J. Geophys. Res.*, **97**, 15 787–15 801.

Duan, J., M. Bevis, P. Fang, Y. Bock, S. Chiswell, S. Businger, C. Rocken, F. Solheim, T. Hove, R. Ware, S. McClusky, T.A. Herring and R.W. King, 1996: GPS meteorology: Direct estimation of the absolute value of precipitable water. *J. Appl. Meteor.*, **35**, 830–838.

Ichikawa, R., M. Kasahara, N. Mannoji and I. Naito, 1995: Estimations of atmospheric excess path delay based on three–dimentional numerical prediction model data. *J. Geod. Soc. Japan*, **41**, 379–408.

———, ———, ——— and ———, 1996: Positioning errors in GPS measurements due to atmospheric excess path delay estimated from three–dimentional, numerical prediction model data. *J. Geod. Soc. Japan*, **42**, 183–204.

Iwasaki, H. and Y. Ohbayashi, 1998: Some characteristic features of hailstorm over Gunma Prefecture, Japan. *Tenki*, **45**, 695–705 (in Japanese).

———, 1999: Case study on the distribution of precipitable water associated with local circulation using the split–window data of a NOAA satellite. *J. Meteor. Soc. Japan*, **77**, 711–719.

Kimata, F., N. Kato and T. Sugimaya, 1996: GPS Measurements Errors for Nagoya–Atsumi Baseline at the Passing of Cold Front on November 7, 1995. *J. Geod.*

Soc. Japan, **42**, 119–122 (in Japanese with English abstract) .

——— and N. Mannoji, 1998: The influence of the atmospheric delay on the accuracy of geodetic parameter estimations. *Kisho Kenkyu Note*, **192**, 49–59 (in Japanese).

Kimura, F and T. Kuwagata, 1993: Thermally induced wind passing from plain to Basin over a mountain range. *J. Appl. Meteo.*, **32**, 1538–1547.

——— and ———, 1995: Horizontal heat flux over a complex terrain computed using a simple mixed–layer model and a numerical model. *J. Appl. Meteor.*, **34**, 549–558.

——— and Tanikawa, 1997: Diurnal variation of precipitable water on clear days over the Northern Mountains in Kanto Plain. *Tenki*, **44**, 799–807 (in Japanese).

Ohtani, R., H. Tsuji, N. Mannoji, J. Segawa and I. Naito, 1997: Precipitable water vapor observed by Geographical Survey Institute's GPS network. *Tenki*, **44**, 315–325 (in Japanese).

———, 2000: A study on the evaluation of GPS retrieved precipitable water vapor. *Docter Thesis*, Univ. of Tokyo.

Rocken, C., T. Van Hove, J. Johnson, F. Solheim, R. Ware, M. Bevis, S. Businger and S. Chiswell 1995: GPS/STORM–GPS sensing of atmospheric water vapor for meteorology. *J. Atmos. Oceanic Technol.*, **12**, 468–478.

Shoji, Y., K. Aonashi, H. Nakamura, A. Ichiki and H. Seko, 1999: Semi-diurna 1 and 2 to 3 hourly errors of GPS derived precipitable water vapor observed during GPS/MET Japan Summer campaign 1997 in Tsukuba an other observations. *Proc. of the International Symposium on GPS*, Tsukuba, Japan, 02–17.

水蒸気勾配がGPS可降水量の精度に与える影響

岩崎博之
（群馬大学教育学部）
木村富士男
（筑波大学地球科学系）
中川清隆
（上越教育大自然系）
三木貴博
（群馬大学教育学部）
木股文昭
（名古屋大学理学部地震火山研究センター）
島田誠一
（防災科学技術研究所）
中尾　茂
（東京大学地震研究所）

マイクロ波放射計で得られた可降水量を真値と考え、水蒸気勾配がGPS可降水量の精度に与える影響について調査した。GPS可降水量とマイクロ波放射計の観測値と比較すると、相関係数は0.991、rmsは1.93 mであり、二つの可降水量は非常に良く一致した。

GPS可降水量の誤差は、変動の時間スケールから、二つの種類に分類された。一つの誤差は、数日の時間スケールで変動し、その振幅は2.5 mmであり、GPS観測点周辺の水蒸気勾配の大きさと有意な相関があった。もう一つの誤差は寒冷前線や温暖前線の通過に関連して観測される。その誤差は数時間スケールで変動し、その変動幅は最大で10 mmであった。この評価誤差は、水蒸気勾配の大きさそのものではなく、急激な水蒸気勾配の変化と対応していた。